ACS Medicinal Chemistry Letters

Letter

Cite This: ACS Med. Chem. Lett. 2018, 9, 528−533

Strategy for Extending Half-life in Drug Design and Its Significance

Hakan Gunaydin,*[,†] Michael D. Altman,[†] J. Michael Ellis,[‡,§] Peter Fuller,[‡] Scott A. Johnson,[†] Brian Lahue,[†] and Blair Lapointe[‡]

[†]Department of Modeling & Informatics and [‡]Department of Medicinal Chemistry, Merck & Co., Inc., 33 Avenue Louis Pasteur, Boston, Massachusetts 02115 United States

Supporting Information

ABSTRACT: Preclinical optimization of compounds toward viable drug candidates requires an integrated understanding of properties that impact predictions of the clinically efficacious dose. The importance of optimizing half-life, unbound clearance, and potency and how they impact dose predictions are discussed in this letter. Modest half-life improvements for short half-life compounds can dramatically lower the efficacious dose. The relationship between dose and half-life is nonlinear when unbound clearance is kept constant, whereas the relationship between dose and unbound clearance is linear when half-life is kept constant. Due to this difference, we show that dose is more sensitive to changes in half-life than changes in unbound clearance when half-lives are shorter than 2 h. Through matched molecular pair analyses, we also show that the strategic introduction of halogens is likely to increase half-life and lower projected human dose even though increased lipophilicity does not guarantee extended half-life.

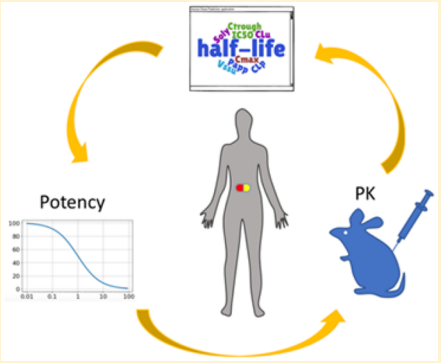

KEYWORDS: *PK, half-life extension, dose prediction, MMP*

In drug discovery, a primary goal of the lead optimization process is to identify a drug candidate. Progression of lead molecules toward improved drug-like space requires optimization of potency and ADMET properties in an iterative manner. The simultaneous optimization of all desired end points frequently poses a challenge for medicinal chemistry teams during the exploration of structure−activity relationships. Hence, medicinal chemists often need some compromise in finding an acceptable balance between potency and desired ADMET properties. The trade-off between potency and pharmacokinetics (PK) is one of the most impactful as they determine the projected human dose to achieve the targeted exposures for clinical evaluations.[1] It is important to highlight that structural modifications may result in changes to multiple end points, and the impact of experimental variability should be minimized by either increasing the number of replicas or increasing the number of observations that support the same conclusion.

The success and the limitations of predicting human PK from preclinical species[2−6] and the benefits of making early human dose predictions[7] are well documented in the literature. While making such early human dose predictions, unbound potency ($IC_{50,u}$) is often used as a surrogate for the desired degree of target coverage at either 12 or 24 h (C_{trough}-based target coverage hypothesis) prior to the elucidation of the PK/PD relationship, and especially for rank ordering compounds. The dose required to cover $IC_{50,u}$ (nM) may be described by the relationship shown in eq 1 for a C_{trough}-based target coverage hypothesis where V_{ssu} (L/kg) is the unbound volume of distribution at steady state, CL_p (mL/min/kg) is the plasma clearance, V_d (L/kg) is the volume of distribution, F is bioavailability, and MW is the molecular weight.[8,9] Predicted human PK parameters can then be used to estimate the dose needed to cover the $IC_{50,u}$ at 12 or 24 h for BID or QD dosing, respectively. Enabling such human dose calculations during the compound optimization stage improves the visibility of the assumptions made for medicinal chemists, and the simplicity of such a model allows teams to devise an effective optimization strategy and focus on improving parameters that are most beneficial for lowering projected human dose. For example, in one chemical series, medicinal chemists may prioritize half-life optimization, whereas in a different chemical series for the same target, they may decide to focus on optimizing potency or unbound clearance in order to have the greatest impact on the projected human dose.

$$\text{dose}_{\text{QD[BID]}} \approx \frac{V_{ss,u}\text{IC}_{50,u}\text{MW}(e^{0.693\times 24[12]/t_{\text{halfeff}}} - 1)}{F};\quad t_{\text{halfeff}} = \ln(2)\frac{V_d}{\text{CL}_p} \tag{1}$$

According to eq 1, the modulation of effective half-life (t_{half_eff}) is an important aspect of optimizing dose since the changes in t_{half_eff} exponentially change the predicted dose, while the changes in all other parameters result in linear changes. Figure 1 illustrates the relationship between half-life

Special Issue: Med Chem Tech: Driving Drug Development

Received: January 12, 2018
Accepted: April 2, 2018
Published: April 2, 2018

DOI: 10.1021/acsmedchemlett.8b00018
ACS Med. Chem. Lett. 2018, 9, 528−533

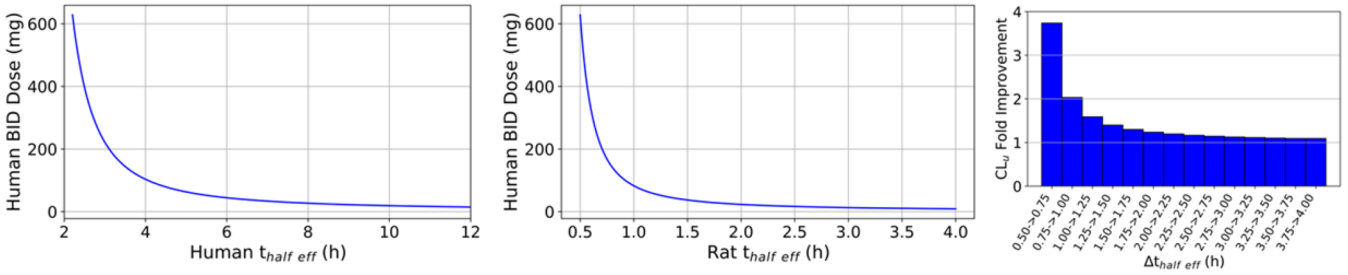

Figure 1. Relationship between predicted human BID dose and human effective half-life (left) and projected relationship between rat effective half-life and human BID dose based on allometric scaling principles (middle). Fold improvement in CL_u that will lower the dose by the same amount as increasing rat half-life by 15 min (right). In the right plot, the first bar represents that ~4-fold improvement in CL_u with no change in rat half-life has the same benefit as not changing CL_u but increasing the half-life by 15 min.[9,10]

and predicted dose for human. Hence, it is important to achieve human half-lives that are amenable to QD or BID dosing for patient compliance and safety reasons since short half-lives will necessitate high peak-to-trough ratios and/or frequent dosing. The significance of t_{half_eff} optimization has been recently reviewed in the literature.[8]

Assuming allometric principles, t_{half_eff} for small molecules is about 4.3 times longer in human than in rat.[2] Hence, one can estimate human t_{half_eff} by multiplying rat t_{half_eff} by 4.3 or relate the projected human dose to rat t_{half_eff} by using this scaling factor. The projected relationship between estimated human dose (for BID dosing) and rat t_{half_eff} is shown in the middle panel of Figure 1. It is easy to factor in the impact of losing 2-fold potency or having lower bioavailability due to the linearity in eq 1. However, the relationship between rat t_{half_eff} and dose is harder to estimate and variable along the range of possible values of half-life. Figure 1 shows that there is a very steep relationship between the projected human dose and rat t_{half_eff} when rat half-lives are short (less than 1 h) and starts to level off when the rat t_{half_eff} extends to more than 2 h for BID dosing. This plot highlights the importance of improving rat t_{half_eff} to beyond 2 h for a C_{trough} driven target for BID dosing based on allometric principles. BID dose may be improved by about 30-fold upon extending the rat half-life from 0.5 to 2 h (4-fold improvement in half-life) even if the unbound clearance remained the same (about 7-fold improvement when half-life changes from 0.5 to 1 h and about 2-fold improvement when rat half-life changes from 1 to 1.5 h). In general, the shorter the half-life, the more sensitive the dose is to absolute changes in half-life.[10]

The bar chart in Figure 1 illustrates the interplay between rat *in vivo* unbound clearance (CL_u)[11] and rat half-life on predicted dose for low extraction ratio compounds; bars represent fold improvement in CL_u that would lower the dose by the same amount as extending rat half-life by 15 min. For example, extension of rat half-life from 0.5 to 0.75 h (with no change in CL_u) lowers the dose by about 4-fold; this predicted improvement in dose may also be achieved by approximately 4-fold improvement in CL_u (first bar in Figure 1 with no change in half-life). This highlights the importance of half-life optimization over CL_u optimization when rat half-lives are extremely short. However, when rat half-life reaches 2 h, extending it no longer has a benefit over reducing CL_u (improvements in half-life and CL_u lower the dose by about the same magnitude). This suggests that it is crucial to increase the half-life, even if it comes at the expense of increased unbound clearance, when the t_{half_eff} is short for compounds with low V_d. It is not recommended to increase the V_d to high values for the reasons explained in detail in a recent review by Smith et al.[8] However, once the rat t_{half_eff} reaches 2 (4) hours (the point of diminishing returns for BID (QD) dosing), there is no room for such a trade-off and one must maintain long half-lives while reducing unbound clearance in order to lower the projected human dose for the same potency. Therefore, dose is as sensitive to CL_u optimization when half-lives are long, whereas in the cases of short half-lives, optimizing t_{half_eff} may be more beneficial. It is important to highlight here that dose predictions made for AUC-based (eq 2) and C_{trough}-based target coverage hypotheses start converging to similar values (less than 2-fold difference) when rat half-lives are longer than 1.5 (3) h for BID (QD) dosing (Figure 2). Hence, lowering CL_u

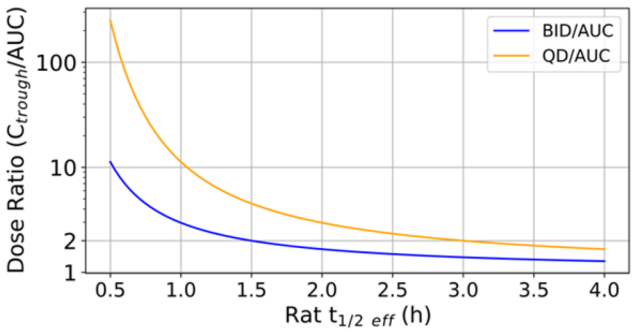

Figure 2. Ratio of human dose predictions made with C_{trough} and AUC-based target coverage hypotheses as a function of rat half-life.

will lower the projected human dose regardless of how the target coverage strategy was set. However, in the cases where t_{half_eff} is short, dose may be more responsive to changes in half-life than changes in CL_u.

$$\text{dose}_{AUC} \approx IC_{50,u} \times MW \times CL_u/F \quad (2)$$

Chemical modifications of molecules may result in increasing CL_u and V_{ssu} proportionally. As seen in Figure 3, measured rat *in vivo* CL_u and V_{ssu} are highly correlated for a set of more than 10,000 MSD molecules with low extraction ratios. Since t_{half_eff} is the ratio of these two parameters, t_{half_eff} often remains approximately the same as CL_u is reduced. Hence, it is important to identify trends that move molecules away from the linear regression line (in favor of increasing V_{ssu} or lowering CL_u) in Figure 3 since t_{half_eff} improves only in such cases.

Matched molecular pairs (MMP) are pairs of molecules that differ by a single chemical transformation and are used to relate the changes in measured activities to changes in chemical structures.[12] One may choose to interrogate the impact of

DOI: 10.1021/acsmedchemlett.8b00018
ACS Med. Chem. Lett. 2018, 9, 528−533

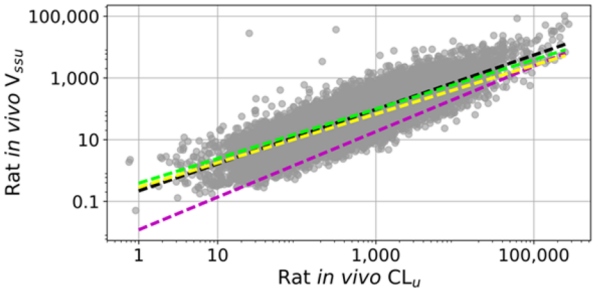

Figure 3. Relationship between unbound *in vivo* CL_u (mL/min/kg) and V_{ssu} (L/kg). Yellow and green lines represent best fit lines H → F MMP transformation, respectively. Black and magenta lines represent best fit lines for H → COOH MMP transformation, respectively.

increased lipophilicity on half-life by comparing hydrogen/fluorine MMPs. MSD PK data was analyzed in order to identify such trends. Yellow and green lines in Figure 3 represent best fit lines for a set of MMPs that correspond to hydrogen to fluorine transformation, respectively. As can be seen in this plot, F analogs have slightly longer t_{half_eff} than the corresponding H analogs. Another MMP example in Figure 3 is the comparison between black (H analog) and red (COOH analog) best fit lines that show that COOH analogs tend to have shorter t_{half_eff} than the corresponding H analogs. These two MMP transformation pairs highlight that lowering CL_u does not necessarily translate to increased t_{half_eff} and short half-lives may hamper the progressability of key molecules even after CL_u optimization if high C_{max}/C_{trough} ratios are not desirable. Smith and co-workers have highlighted the importance of V_d and half-life optimization in drug design and also speculated that the increase in nonmetabolizable lipophilicity may afford half-life extension in a recent perspective article.[13]

One can increase t_{half_eff} by increasing the amount of compound that partitions into tissue. One way to achieve this is to increase the lipophilicity of molecules. Since an increase in lipophilicity is also likely to increase PPB, in this strategy, one is aiming to increase the tissue binding to a larger extent than PPB upon increasing lipophilicity. Figure 4 shows the analysis of H → F MMP transformation when one, two, or three hydrogen atoms were replaced with fluorine atoms. The sequential addition of fluorine atoms to the molecules statistically significantly increases t_{half_eff} (Table 1). This analysis suggests that t_{half_eff} may be improved by adding halogens to molecules, and the extent by which t_{half_eff} improves is proportional to the number of halogens added to the molecules. This observed trend is presumably due to the increased propensity of halogenated molecules in Table 1 for nonspecific binding. Since there is more tissue in the body than albumin, the increase in lipophilicity presumably increased PPB to a lesser extent than it did tissue binding as halogens were added to molecules resulting in increased t_{half_eff}.

It is interesting to note that measured t_{half_eff} did not improve when the hydrogen atom was replaced with a methyl group (Figure S1 and Table 1). This suggests that the improvement in t_{half_eff} was only observed when metabolically inert lipophilicity was added to the molecules. In order to validate this hypothesis, H → Cl, H → CF_3, and Me → Cl MMPs were also analyzed (Figure S1 and Table 1). H → Cl and H → CF_3 MMP analyses represent cases in which nonmetabolizable lipophilicity was added to the molecules, and one would assume that the increase in lipophilicity may help improve measured t_{half_eff} in these cases despite the fact that increased lipophilicity may also increase the overall rate of metabolism at other positions of molecules. The last MMP analysis (Me → Cl) represents the case in which both molecules have about the same lipophilicity, and methyl analogs may present metabolic soft spots, whereas Cl analogs may not. All of these transformations indeed increased t_{half_eff}. The increase in the H → Cl and H → CF_3 MMPs could be attributed to the increase in lipophilicity, whereas the increase in t_{half_eff} with the Me → Cl transformation may be partly attributed to the elimination of metabolic soft spots since both Me and Cl analogs have similar cLogP values. Hence, half-life extension may be achieved through either blocking of the metabolism or the increase in metabolically inert lipophilicity.

Further analysis of the MSD *in vivo* CL_u and V_{ssu} data for these MMPs revealed that both the median unbound clearance and median unbound volume went up for all these transformations; in cases where half-life improved, it was observed that median V_{ssu} increased more than median CL_u (Table S1 and Figure S1). It is interesting to note here that the median *in vivo* CL_u increased when Me group was replaced with a Cl atom. However, median *in vivo* V_{ssu} increased even more and resulted in half-life extension in this MMP transformation (Table S1). It is also important to recognize that increased lipophilicity may decrease the solubility of molecules and may pose a development risk.[14]

In order to support the findings presented here, additional MMP transformations in which hydrogen was replaced with a more polar functional group were analyzed. If the hypothesis presented here (increase in nonspecific binding increases half-life) were to be true, one would assume that the transformations in which hydrogen is replaced with more polar group should shorten t_{half_eff}. Indeed, we observed that phenyl → pyridine and H → OH transformations shortened measured half-lives by 0.20 and 0.28 h, respectively (Table 1 and Figure S2). There were 79 H → COOH transformations that showed that carboxylic acid analogs, on average, had 0.74 h shorter half-lives. This transformation represents an interesting scenario since COOH analogs tend to have higher PPB due to their

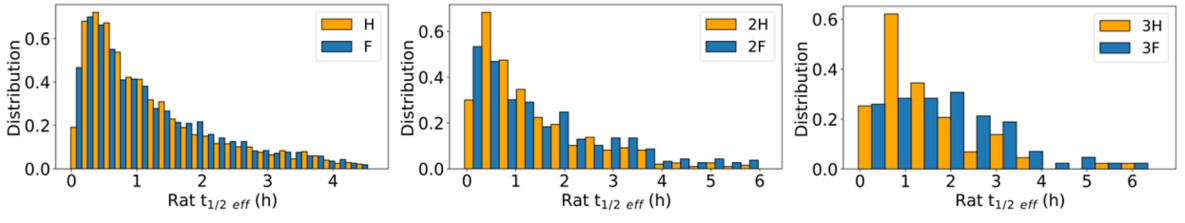

Figure 4. Matched molecular pair (MMP) analyses that show the improvement in measured rat effective half-lives upon sequential H → F transformations.

DOI: 10.1021/acsmedchemlett.8b00018
ACS Med. Chem. Lett. 2018, 9, 528−533

Table 1. Statistics of Half-Life Change for MMP Analyses[a]

MMP	Δt_{half} (h)	*p*-value	*N*	MMP	Δt_{half} (h)	*p*-value	*N*
H → F	+0.12	2.7×10^{-6}	4539	H → CF_3	+0.34	9.9×10^{-10}	524
2H → 2F	+0.35	4.2×10^{-5}	573	Me → Cl	+0.21	4.7×10^{-5}	555
3H → 3F	+0.99	4.9×10^{-5}	78	Ph → Py	−0.20	6.8×10^{-11}	2419
H → Me	+0.00	0.72	5377	H → OH	−0.28	7.9×10^{-9}	595
H → Cl	+0.27	2.8×10^{-9}	1255	H → COOH	−0.74	9.8×10^{-9}	79

[a]*N* corresponds to number of MMPs.

affinity to albumin.[15−17] This suggests that an increase in PPB is not responsible for the observed increase in half-life with halogenated analogs in Figures 4 and S1, and the increase in tissue binding affords half-life extension. The analysis of *in vivo* clearance and volume data (Table S1) revealed that the median unbound clearance went down for all of these transformations as one might expect. However, V_{ssu} decreased to a larger extent and resulted in shortened half-lives.

In order to generalize the observations exemplified with MMP transformations in Table 1, all possible MMP transformations in which hydrogen is replaced with a substituent that either increases or decreases Biobyte cLogP of molecules were analyzed (Figure 5). In this MMP analysis, all possible

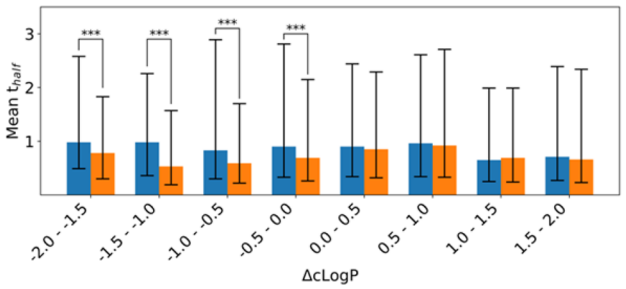

Figure 5. Bar charts that highlight the relationship between the change in half-life and change in cLogP upon replacement of a hydrogen atom with a substituent. Blue bars correspond to hydrogen analogs, and orange bars correspond to substituted analogs. Lines represent the range of one standard deviation, and statistically significant changes are highlighted.

substitutions were considered and binned with respect to how much the substituent changes cLogP of the hydrogen containing reference molecule (ΔcLogP). For example, all aromatic H → F and aliphatic H → Cl pairs were included in the ΔcLogP 0−0.5 bin, whereas aliphatic H → F pairs were included in the ΔcLogP −0.5−0 bin, and aromatic H → Cl transformations were included in ΔcLogP 0.5−1.0 bin. In Figure 5, half-life distributions of substituted analogs (orange bars) were compared to reference hydrogen analogs within the same bin (blue bars), and the changes that are statistically significant were highlighted. As seen in Figure 5, the increase in overall lipophilicity does not necessarily correspond to increased half-life, and a decrease in lipophilicity appears to correlate with shortened half-life. These results are in contrast with the MMP observations exemplified in Table 1 and highlight the limitations of overgeneralized trends. For example, a decision to lower the lipophilicity in an attempt to increase half-life may result in decreasing half-life.

Further analysis of rat *in vivo* CL_u and *in vivo* V_{ssu} revealed that the observed improvement in half-life, in cases where it was statistically significant, was achieved despite the increase seen in *in vivo* CL_u (Table S1 and Figure S3); a disproportionately larger increase in V_{ssu} relative to that of observed *in vivo* CL_u was responsible for the half-life extension. This, in addition to the observations seen in MMPs, suggests that V_{ssu} is more sensitive to the chemical modifications that impact lipophilicity, presumably due to the fact that V_d spans a smaller range relative to the range of values observed in CL_p and that disproportionate changes in these two values result in changes observed in half-life.

MSD PK data was further analyzed in order to identify privileged functional groups that are observed in increased propensity in low *in vivo* CL_u (*in vivo* CL_u values that are less than mean minus two standard deviations) and long half-life (rat t_{half_eff} greater than 2 h) compounds with low extraction ratios. Some of the fragments that have increased propensity to have low *in vivo* CL_u and long t_{half_eff} are shown in blue in Figure 6. Halogenated and basic amine containing fragments

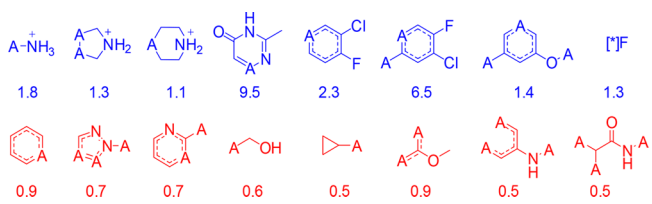

Figure 6. Fragments observed in increased propensity in low *in vivo* CL_u and long t_{half_eff} compounds (in blue) and high *in vivo* CL_u and short t_{half_eff} compounds (in red). A represents any atom. Odds ratios to find these fragments in low *in vivo* CL_u and long t_{half_eff} compounds were also provided under each fragment.

were found to have increased propensity in this set of compounds, whereas the fragments highlighted in red were found to have increased propensity in high *in vivo* CL_u and short t_{half_eff} compounds. Some of the highlighted fragments in Figure 6 corroborate the observations seen in Table 1 and highlight the need to examine holistic trends (such as the ones shown in Figure 5) in addition to specific trends that may have been overlooked in holistic analyses (such as the ones in Table 1) in order to progress molecules to improved drug-like space.

Figure 7 shows example MMPs with measured rat t_{half_eff} and dose projections with allometric principles. The **C1**/**C2** pair illustrates that the addition of a F atom can improve the measured rat t_{half_eff} by 0.37 h. This pair also shows that a greater than 2-fold increase in measured *in vivo* CL_u did not result in any substantial change in dose prediction because of the extended half-life in **C2**.[18] **C3**/**C4** transformation exemplifies a scenario in which the addition of polarity may result in shortened half-life. The comparison of molecules **C2** and **C4** highlights the importance of half-life; **C4**, despite having about 5-fold improved *in vivo* CL_u (relative to **C2**), has less than 2-fold better predicted dose due to its shorter half-life. Structures and PK profiles shown in Figure 7 highlight the importance of understanding the limitations of commonly used

DOI: 10.1021/acsmedchemlett.8b00018
ACS Med. Chem. Lett. 2018, 9, 528−533

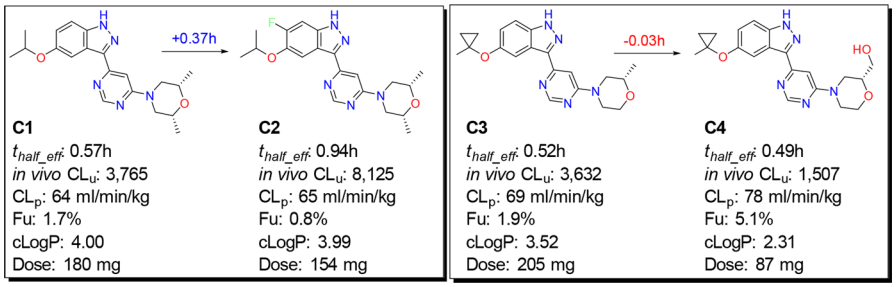

Figure 7. Examples of MMPs that show the change in half-lives upon changing the lipophilicity of the molecules. Molecules **C1** through **C4** have measured bioavailability of 25, 20, 32, and 36%, respectively.

dose optimization strategies and making timely tractability decisions for a given chemical series.

In summary, in medicinal chemistry optimization of lead molecules, it is important to (1) make use of early dose predictions, (2) decide on C_{trough} or AUC driven PK/PD, and (3) identify key parameters that affect those dose predictions.

Tailoring optimization strategies for each chemical series is a useful way to help advance chemical series. Here we show that short t_{half_eff} can hamper the progression of chemical series, even in the cases where low *in vivo* CL_u values are achievable for C_{trough} targets, and present MMPs that improve rat half-lives. Hence, understanding the PK space of the compounds in a given chemical series and making appropriate decisions on what to improve are very important considerations during iterative SAR exploration. Here, we show that increasing lipophilicity could be an effective way of improving t_{half_eff} in situations where short half-lives are hampering the progression of chemical series. In these cases, once such problem is identified; the use of QSAR models[19] may guide medicinal chemists toward identifying positions on molecules where metabolically inert lipophilicity may be added to improve half-lives while ensuring that unbound clearance remains low.

■ ASSOCIATED CONTENT

Supporting Information

The Supporting Information is available free of charge on the ACS Publications website at DOI: 10.1021/acsmedchemlett.8b00018.

Changes in median *in vivo* CL_u and *in vivo* V_{ssu} for the transformation exemplified, half-life change distributions for H → Me, H → Cl, H → CF_3, Me → CF_3, phenyl → pyridine, H → OH, and H → COOH transformations, and the plot of the relationship between *in vivo* clearance and bioavailability (PDF)

■ AUTHOR INFORMATION

Corresponding Author

*E-mail: hakan.gunaydin@merck.com.

ORCID

Hakan Gunaydin: 0000-0003-1093-2787

Present Address

§Medicinal Chemistry, Celgene Corp., 200 Cambridge Park Drive, Cambridge, Massachusetts 02140, United States.

Notes

The authors declare no competing financial interest.

■ ACKNOWLEDGMENTS

Authors would like to thank Andreas Verras, Iain Martin, Charles Lesburg, and John Sanders for useful discussions.

■ ABBREVIATIONS

PK, pharmacokinetics; CL_u, unbound clearance; CL_{int}, intrinsic clearance; V_{ssu}, unbound volume of distribution at steady state; $t_{half\ eff}$, effective half-life; MMP, matched molecular pair; V_d, volume of distribution; CL_p, plasma clearance; QD, once daily; BID, twice a day; PPB, plasma protein binding; *F*, bioavailability; MW, molecular weight; hF_u, fraction unbound in human plasma; cLogP, calculated octanol/water partition coefficient; $IC_{50,u}$, unbound concentration of inhibitor to achieve 50% reduction in activity; C_{max}, maximum plasma concentration; C_{trough}, plasma concentration prior to administration of next dose; SAR, structure−activity relationship

■ REFERENCES

(1) Kola, I.; Landis, J. Can the pharmaceutical industry reduce attrition rates? *Nat. Rev. Drug Discovery* **2004**, *3*, 711−715.

(2) Caldwell, G. W.; Masucci, J. A.; Yan, Z.; Hageman, W. Allometric scaling of pharmacokinetic parameters in drug discovery: can human CL, Vss and t1/2 be predicted from in-vivo rat data? *Eur. J. Drug Metab. Pharmacokinet.* **2004**, *29*, 133−143.

(3) Hosea, N. A.; Collard, W. T.; Cole, S.; Maurer, T. S.; Fang, R. X.; Jones, H.; Kakar, S. M.; Nakai, Y.; Smith, B. J.; Webster, R.; Beaumont, K. Prediction of human pharmacokinetics from preclinical information: comparative accuracy of quantitative prediction approaches. *J. Clin. Pharmacol.* **2009**, *49*, 513−533.

(4) Tang, H.; Hussain, A.; Leal, M.; Mayersohn, M.; Fluhler, E. Interspecies prediction of human drug clearance based on scaling data from one or two animal species. *Drug Metab. Dispos.* **2007**, *35*, 1886−1893.

(5) Tang, H.; Mayersohn, M. A novel model for prediction of human drug clearance by allometric scaling. *Drug Metab. Dispos.* **2005**, *33*, 1297−1303.

(6) Yang, J.; Jamei, M.; Yeo, K. R.; Rostami-Hodjegan, A.; Tucker, G. T. Misuse of the well-stirred model of hepatic drug clearance. *Drug Metab. Dispos.* **2007**, *35*, 501−502.

(7) Page, K. M. Validation of Early Human Dose Prediction: A Key Metric for Compound Progression in Drug Discovery. *Mol. Pharmaceutics* **2016**, *13*, 609−620.

(8) Smith, D. A.; Beaumont, K.; Maurer, T. S.; Di, L. Relevance of Half-Life in Drug Design. *J. Med. Chem.* **2017**, DOI: 10.1021/acs.jmedchem.7b00969.

(9) Wagner, J. G.; Northam, J. I.; Alway, C. D.; Carpenter, O. S. Blood Levels of Drug at the Equilibrium State after Multiple Dosing. *Nature* **1965**, *207*, 1301−1302.

(10) In order to make human dose projections, it was assumed that the theoretical compound is 5 nM (unbound) against its target with a molecular weight of 450 Da, PPB of 99% in both rat and human, rat volume of distribution (V_d) of 0.7 L/kg and bioavailability (F) of

DOI: 10.1021/acsmedchemlett.8b00018
ACS Med. Chem. Lett. 2018, 9, 528−533

100%. It should be recognized that these assumed PK parameters may change disproportionately upon compound optimization. The relationship between *in vivo* clearance and bioavailability is provided in the SI in support of the use of equal bioavailability.

(11) CL_{int} and CL_u are calculated with the formulae $CL_p/f_u \times (Q/(Q - CL_p))$ and CL_p/f_u, respectively. Q corresponds to rate of hepatic blood flow to the liver. For compounds with low-to-moderate extraction ratio, CL_{int} and CL_u are approximately the same.

(12) Kramer, C.; Ting, A.; Zheng, H.; Hert, J.; Schindler, T.; Stahl, M.; Robb, G.; Crawford, J. J.; Blaney, J.; Montague, S.; Leach, A. G.; Dossetter, A. G.; Griffen, E. J. Learning Medicinal Chemistry Absorption, Distribution, Metabolism, Excretion, and Toxicity (ADMET) Rules from Cross-Company Matched Molecular Pairs Analysis (MMPA). *J. Med. Chem.* **2017**, DOI: 10.1021/acs.jmedchem.7b00935.

(13) Smith, D. A.; Beaumont, K.; Maurer, T. S.; Di, L. Volume of Distribution in Drug Design. *J. Med. Chem.* **2015**, *58*, 5691−5698.

(14) Wuelfing, W. P.; Daublain, P.; Kesisoglou, F.; Templeton, A.; McGregor, C. Preclinical dose number and its application in understanding drug absorption risk and formulation design for preclinical species. *Mol. Pharmaceutics* **2015**, *12*, 1031−1039.

(15) Bhattacharya, A. A.; Grune, T.; Curry, S. Crystallographic analysis reveals common modes of binding of medium and long-chain fatty acids to human serum albumin. *J. Mol. Biol.* **2000**, *303*, 721−732.

(16) Sudlow, G.; Birkett, D. J.; Wade, D. N. The characterization of two specific drug binding sites on human serum albumin. *Mol. Pharmacol.* **1975**, *11*, 824−832.

(17) Vallner, J. J. Binding of drugs by albumin and plasma protein. *J. Pharm. Sci.* **1977**, *66*, 447−465.

(18) In order to make dose predictions for the molecules shown in Figure 7 for easier comparison, we assumed that all molecules had the same unbound potency and bioavailability. Biochemical potencies measured against their targets for these molecules ranged from 0.7 to 2 nM.

(19) Svetnik, V.; Liaw, A.; Tong, C.; Culberson, J. C.; Sheridan, R. P.; Feuston, B. P. Random forest: a classification and regression tool for compound classification and QSAR modeling. *J. Chem. Inf. Comput. Sci.* **2003**, *43*, 1947−1958.

DOI: 10.1021/acsmedchemlett.8b00018
ACS Med. Chem. Lett. 2018, 9, 528−533